NJC

Accepted Manuscript

This is an *Accepted Manuscript*, which has been through the Royal Society of Chemistry peer review process and has been accepted for publication.

Accepted Manuscripts are published online shortly after acceptance, before technical editing, formatting and proof reading. Using this free service, authors can make their results available to the community, in citable form, before we publish the edited article. We will replace this *Accepted Manuscript* with the edited and formatted *Advance Article* as soon as it is available.

You can find more information about *Accepted Manuscripts* in the Information for Authors.

Please note that technical editing may introduce minor changes to the text and/or graphics, which may alter content. The journal's standard Terms & Conditions and the Ethical guidelines still apply. In no event shall the Royal Society of Chemistry be held responsible for any errors or omissions in this *Accepted Manuscript* or any consequences arising from the use of any information it contains.

ROYAL SOCIETY OF CHEMISTRY

www.rsc.org/njc

Dual role of Lewis acid and base for pnicogen and unexpected interplay between pnicogen bond and coordination interaction in $H_3N\cdots FH_2X\cdots MCN$ (X = P and As; M = Cu, Ag, and Au)

Hongying Zhuo, Qingzhong Li*, Wenzuo Li, Jianbo Cheng

The Laboratory of Theoretical and Computational Chemistry, School of Chemistry and Chemical Engineering, Yantai University, Yantai 264005, People's Republic of China

Corresponding author:

Qingzhong Li Dr

The Laboratory of Theoretical and Computational Chemistry

School of Chemistry and Chemical Engineering

Yantai University

Yantai 264005

People's Republic of China

Tel. (+086) 535 6902063

Fax. (+086) 535 6902063

E-mail: liqingzhong1990@sina.com

Abstract

Ternary systems $H_3N\cdots FH_2X\cdots MCN$ (X = P and As; M = Cu, Ag, and Au) as well as the corresponding pnicogen-bonded and coordination-bonded binary systems have been studied. The X atom respectively acts as the electron acceptor and donor in the pnicogen bond and coordination interaction, simultaneously playing both roles in the ternary complexes. Electrostatic interaction and charge transfer have dominant contribution to the stability of pnicogen bond, while the origin of coordination interaction results mainly from electrostatic and polarization interactions. Relativistic effects especially for Au atom lead to some irregularity of interaction energy and binding distance in the coordination interactions. In the ternary complex, the stronger coordination interaction strengthens the weaker pnicogen bond, while the pnicogen bond weakens the coordination interaction. The weakening of the coordination interaction was evidenced by the longer binding distance, lower electron density at the bond critical point, and smaller charge transfer. The change of pnicogen bond and coordination interaction in the ternary complex has been rationalized with the analyses for the electrostatic potentials, occupancy on the lone pair of X atom as well as the orbital interactions.

Keywords: Pnicogen bond; Coordination interaction; Interplay

1. Introduction

Pnicogen bond, a new type of intermolecular interaction, has drawn more and more attentions from both theoretical and experimental researchers since Hey-Hawking *et al*. thought it may be a new molecular linker in crystal meterials.[1] Particularly, many theoretical studies have been performed for pnicogen-bonded binary complexes involving H_3P and its derivatives.[2-21] Usually, the electron donors of pnicogen bonds were lone pairs from molecules such as NH_3, although other types of electron donors were also used.[12-21] The electrostatic contribution to the formation of pnicogen bond was described in terms of the σ−hole concept proposed by Politzer and Murray.[22] This σ−hole refers to the electron-deficient outer lobe of a *p* orbital of an electronegative atom. On the other hand, Scheiner ascribed this attraction in part to the transfer of electron density from the lone pair of the electron donor atom to the anti-bond orbital of a P–X covalent bond.[5] It was shown that the strengths of pnicogen bonds are related not only with the nature of pnicogen atoms[23-28] but also with effects of substitution[29-31] and hybridization,[24-28] exhibiting similar effects with hydrogen bonds.[32] Importantly, the strengths of pnicogen bonds determine the stability, nature, and properties of pnicogen-bonded complexes. For example, when the interaction energy of pnicogen bond varies from -1.4 kcal/mol of $H_3P\cdots NH_3$ complex to -43.2 kcal/mol of $FH_2P\cdots F^-$, this interaction exhibits a nature of partially covalent bond.

Additionally, some ternary complexes involving FH_2P were also studied to regulate the strength of pnicogen bond by combining it with other types of interactions.[14,33-37] $HF\cdots FH_2P\cdots FH_2N$ complex shows a synergistic effect between pnicogen and hydrogen

bonds when F−H···F hydrogen bond forms at P−F but a diminutive one when hydrogen bonding occurs at N−F.[33] The similar effects were also found for other ternary complexes where pnicogen and hydrogen bonding interactions coexist.[14,34,35] Pnicogen bonding was enhanced by halogen bonding in $XCl\cdots FH_2P\cdots NH_3$ (X = F, OH, CN, NC, and FCC), depending on the strength of halogen bonding.[36] Very recent, we paid our attention to the cooperative and diminutive effects of pnicogen bond and cation-π interaction.[37]

It was demonstrated that halogen acts as a dual role of Lewis acid and base in triangular halogen trimers $(RX)_3$ (X = Br, I; R = H, H_3C, H_2FC, HF_2C, F_3C, CH_2=CH, CH≡C, and Ph)[38] as well as in ring-shaped trimers $H_3N\cdots X(Y)\cdots HF$ (X = Cl and Br; Y = F, Cl, and Br),[39] where the halogen atom serves as halogen-bonding donor and hydrogen-bonding acceptor simultaneously. Similarly, the dual role of Lewis acid and base was also found for the pnicogen atom in homotrimers $(PH_3)_3$[40] and $(PH_2X)_3$ with X = F, Cl, OH, NC, CN, CH_3, H, and BH_2[41] as well as in heterotrimers $LA\cdots FH_2P\cdots FH_2N$ and $LA\cdots H_3P\cdots NH_3$ (LA = BH_3, NCH, ClH, FH, FCl, and HLi).[42] The dual roles of Lewis acid and base for both halogen and pnicogen atoms are attributed to the presence of the σ-hole and lone pair on both types of atoms.

Inspired by the above results, we designed the ternary systems $H_3N\cdots FH_2X\cdots MCN$ (X = P and As; M = Cu, Ag, and Au), where FH_2X and NH_3 are combined with a pnicogen bond as well as MCN and FH_2X are bonded through a coordination interaction. The σ-hole and lone pair on X are taken as the Lewis acid and base in the pnicogen bond and coordination interaction, respectively. It was known that PH_3 and its

derivatives as a ligand donate electrons to metal compounds and complexes with luminescence and phosphorescence.[43] Hence, we considered the influence of pnicogen bond on the structure, nature, strength, and properties of coordination interaction on the base of model metal compound MCN. On the other hand, our aim is to strengthen the pnicogen bond through the cooperative effect with the coordination interaction, which is much stronger than non-covalent interactions.

2. Computational details

The geometries of monomers and complexes were optimized first at MP2/aug-cc-pVDZ level and then at the MP2/aug-cc-pVTZ level for all atoms except the coinage metal atoms (Cu, Ag, and Au), for which the basis set aug-cc-pVTZ-PP[44] was used to account for relativistic effects. Harmonic vibrational frequency calculations were performed at the same level to verify that the optimized structures correspond to the ground state local minimum. Interaction energies were calculated using the supermolecular method as the difference between the energy of the complex and the energy sum of the isolated monomers. The interaction energies were corrected for the basis-set superposition error (BSSE) using the standard counterpoise method of Boys and Bernardi. [45] All calculations were performed via the Gaussian 09 set of codes.[46]

The wavefunction obtained at the MP2/aug-cc-pVDZ level was used to calculate the molecular electrostatic potentials (MEPs) at the 0.001 electrons $Bohr^{-3}$ isodensity surfaces with the Wave Function Analysis-Surface Analysis Suite (WFA-SAS) program,[47] the electron density (ρ), Laplacian ($\nabla^2\rho$), and energy density (H) at bond critical points (BCPs) in the complexes using AIM2000 program,[48] as well as the

change of electron density with Multiwfn program.[49] Nature bond orbital (NBO) analysis[50] was carried out to explore charge transfer and orbital interactions using NBO6.0 program at the HF/aug-cc-pVTZ level. To gain an insight into the nature of the pnicogen bond and coordination interaction, the localized molecular orbital energy decomposition analysis (LMOEDA) method[51] within GAMESS program[52] was performed at the MP2/aug-cc-pVDZ level. Total interaction energy was decomposed into five components with clearly physical pictures: electrostatic energy (ES), exchange energy (EX), repulsion energy (REP), polarization energy (POL), and dispersion energy (DISP).

3. Results and discussion

3.1. FH_2X (X = P, As) respectively acting as the electron acceptor and donor

Fig. 1 is the schemes of pnicogen-bonded and coordination-bonded binary systems with the X atom of FH_2X (X = P and As) acting as the electron acceptor and donor to interact with NH_3 and MCN, respectively. These structures exhibit C*s* symmetry. The interaction energies, binding distances, and bond angles in these complexes are illustrated in Table 1. Our result for the interaction energy (-6.5 kcal/mol) of $FH_2P\cdots NH_3$ is close to that reported by Del Bene *et al*. at the MP2/aug'-cc-pVTZ level (about -7.1 kcal/mol).[53] The interaction energies were also obtained with a single point energy calculation at the CCSD(T)/aug-cc-pVTZ level on the MP2 geometries. As expected, the MP2 method overestimates the interaction energies of pnicogen bond and coordination interaction relative to the CCSD(T) results. The overestimation is -0.5 kcal/mol ~ -10.7 kcal/mol, amounting to about 8.7-32.5% of the CCSD(T) interaction

energy. Also the most overestimation is found in the CuCN complex. However, the variation tendency of the interaction energy is the same for both methods. For the pnicogen-bonded complexes of $FH_2P\cdots NH_3$ and $FH_2As\cdots NH_3$, the variation of the pnicogen atom from P to As results in a shortening of X···N distance (0.005 Å) and an increase of interaction energy (-1.3 kcal/mol). According to the previous studies on pnicogen bonds,[5-9] the formation of pnicogen bonds mainly arises from the electrostatic interaction between the positive charged σ−hole on the pnicogen atom and the lone pair on the nitrogen base as well as the charge transfer from the lone pair on the nitrogen base to the F−X σ* anti-bonding orbital. Evidently, when the electron donor is hold, a larger positive MEP of the σ−hole on the pnicogen atom and a bigger charge transfer will generate a more stable pnicogen-bonded complex. Indeed, the maximum positive MEP of As atom (0.0685 au) in FH_2As is greater than that of P atom (0.0604 au) in FH_2P, shown in Fig. 2; and the charge transfer (Table 1) is 0.0445e and 0.0531e for the P···N and As···N interactions, respectively. The charge transfer to the F−X σ* anti-bonding orbital is responsible for the elongation of the F−X bond and a red shift of the F−X stretch vibration (Table S1). The elongation of the F−As bond is greater than that of the F−P bond, but the former bond displays a smaller red shift than the latter one. The former result is consistent with the strength of pnicogen bond, while the latter one is attributed to the heavier mass of As atom. Unlike halogen bonding, the bond angle F−X···N of pnicogen bond in $FH_2X\cdots NH_3$ is smaller with the increase of the X atomic mass (Table 1). Consistent with the aforementioned two mainly reasons for the formation of pnicogen bond, the similar results are also obtained with energy

decomposition analysis. One can see from Table 2 that electrostatic energy (ES) and exchange energy (EX) in the first and second columns do make a strong contribution to the stabilization of the pnicogen bond. The larger ES corresponds to the strong attraction interaction between the positive σ−hole on the X atom and the lone pair on the N atom, and this term becomes more negative with the increase of the positive MEP on the σ−hole of the X atom. The EX term usually represents the interpenetration of electron clouds of the bonded monomers, and a larger EX is accompanied by a bigger charge transfer between the related molecular orbitals. Compared with ES and EX, the contribution of POL and DISP terms is very small in the pnicogen bonds.

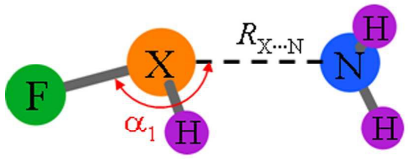

$FH_2X\cdots NH_3$ (X = P and As)

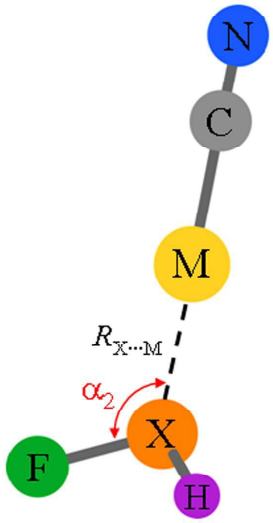

$FH_2X\cdots MCN$
(X = P and As; M = Cu, Ag, and Au)

Fig. 1 Schemes of $FH_2X\cdots NH_3$ (X = P and As) and $FH_2X\cdots MCN$ (X = P and As; M = Cu, Ag, and Au).

Table 1 Interaction energy corrected for BSSE (ΔE, kcal/mol), binding distance (R, Å), angles (α, deg), the sum of charge on all atoms of FH_2X (q, e), second-order perturbation energy (E^2, kcal/mol), electron density (ρ, au) and energy density (H, au) at the intermolecular bond critical point in the heterodimers.

	ΔE	R	α	q_{FH2X}	E^2	ρ	H
$FH_2P\cdots NH_3$	-6.5(-6.0)	2.603	167.8	-0.0596	14.8	0.028	-0.002
$FH_2As\cdots NH_3$	-7.8(-7.2)	2.598	165.2	-0.0675	19.0	0.031	-0.003
$FH_2P\cdots CuCN$	-45.9(-35.2)	2.083	116.6	0.2380	4.7	0.121	-0.071
$FH_2P\cdots AgCN$	-37.5(-29.7)	2.268	115.7	0.2024	4.4	0.106	-0.049
$FH_2P\cdots AuCN$	-58.6(-48.4)	2.202	116.5	0.2850	8.5	0.135	-0.082
$FH_2As\cdots CuCN$	-37.5(-28.3)	2.178	114.9	0.2513	4.5	0.104	-0.054
$FH_2As\cdots AgCN$	-31.5(-24.4)	2.359	114.4	0.2064	4.4	0.092	-0.038
$FH_2As\cdots AuCN$	-49.4(-40.0)	2.304	114.9	0.2917	8.1	0.115	-0.060

Note: α is α_1 and α_2 for $FH_2X\cdots NH_3$ and $FH_2X\cdots MCN$ in Figure 1, respectively. The data in parentheses are the interaction energies with a single point energy calculation at the CCSD(T)/aug-cc-pVTZ level on the MP2 geometries. E^2 corresponds to the orbital interaction of $LP_N\rightarrow BD^*_{F\text{-}X}$ in $FH_2X\cdots NH_3$ and $LP_M\rightarrow BD^*_{F\text{-}X}$ in $FH_2X\cdots MCN$.

Table 2 Energy components and interaction energy (kcal/mol) in the heterodimers

	ES	EX	REP	POL	DISP	E^{int}
$H_3N\cdots FH_2P$	-18.7	-31.1	55.4	-8.2	-4.4	-7.0
$H_3N\cdots FH_2As$	-23.6	-35.3	64.4	-9.7	-4.3	-8.5
$FH_2P\cdots CuCN$	-67.9	-90.2	179.5	-35.7	-24.8	-39.1
$FH_2P\cdots AgCN$	-66.1	-99.9	194.8	-40.4	-16.1	-27.7
$FH_2P\cdots AuCN$	-76.3	-136.9	270.0	-87.7	-18.5	-49.4
$FH_2As\cdots CuCN$	-54.6	-76.7	151.2	-30.8	-23.4	-34.3
$FH_2As\cdots AgCN$	-54.4	-86.2	166.4	-34.7	-16.5	-25.4
$FH_2As\cdots AuCN$	-62.3	-115.6	223.9	-72.5	-19.1	-45.6

When FH_2X (X = P and As) is paired with MCN (M = Cu, Ag, and Au), the lone pair on the X atom of FH_2X is oriented directly to the region of positive MEP on the M atom of MCN (Fig. 2). Clearly, the angle C−M···X is almost 180^o. Interacting with the same metal atom, FH_2P tends to be a better electron donor than FH_2As, characterized by a bigger interaction energy in FH_2P···MCN. Simply, we might ascribe the above variation trend to the negative MEP of the lone pair on the X atom (-0.0190 au for the P atom and -0.0089 au for the As atom). It is natural that the more negative MEP on the nearby of P atom forms a more stable X···M interaction with the same positive charged metal atom. But things seem to be unanticipated for the X···M interaction when the X atom is the same. Paired with the same X atom, AuCN forms a stronger coordination interaction than CuCN, and the latter is a stronger Lewis acid than AgCN, evidenced by the interaction energy. Likely, the metal-π interaction in C_2H_4···MCN (M = Cu, Ag, and Au) complexes also exhibits the same trend in stability.[54] The X···M distance is longer when X is from P to As for the same coinage metal, consistent with the variation of interaction energy. However, this distance becomes longer in the order of Cu < Au < Ag when X is the same, which may be a combination result of the interaction energy and the atomic radius of the coinage metal. The X···M interaction results in a contraction of the F−X bond and a blue shift of this bond stretch vibration (Table S1), which is reverse to that in the pnicogen bond. The change of the C≡N bond is tiny, whereas the M−C bond shows an obvious elongation although its frequency shift is irregular.

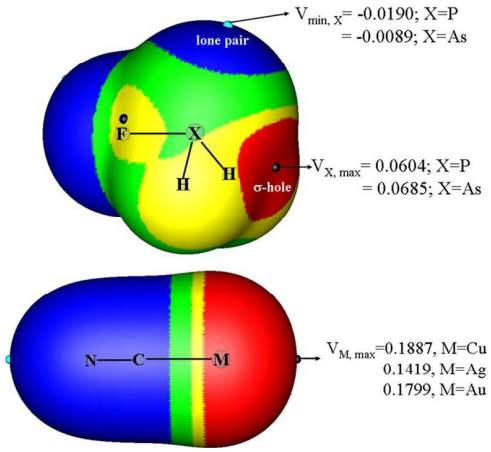

Fig. 2 MEP maps of the monomers with the most positive (V_{max}) and negative (V_{min}) MEPs. Color ranges, in au, are: red, greater than 0.03; yellow, between 0.03 and 0.02; green, between 0.02 and 0; blue, less than 0.

To have a deep understanding of the above unexpected irregularity of interaction energy and the binding distance in $FH_2X\cdots MCN$ complex, a detailed analysis has been performed. Instinctively, we trace back to the nature of MCN (M = Cu, Ag, and Au). Many theoretical studies have been performed to investigate the mechanism of the formation of the noble metal cyanides.[55-59] Noble metal cyanide (MCN) can be treated as a coordination-bonded binary system composed of a noble metal atom and a cyano ligand. It must be noted that relativistic effects have an important effect on the formation of MCN, due to the use of pseudopotential methods for the transition metal elements, especially for Au atom.[58,59] It is shown that the relativistic effects can shorten the M−C distance and this distance is greater in the order of Cu < Au < Ag, which is the same order as the above mentioned binding distance variation for $H_2FX\cdots MCN$ but is different from the regular increasing trend Cu < Ag < Au in the nonrelativistic calculations.[58] As a consequence, it is the relativistic effect that is responsible for the shorter Au−C bond in AuCN. Also the particularity of gold atom is jointly attributed to

the contraction of the 6s atomic orbital, the dilation of the 5d atomic orbital, and the accompanying diminishments of the one electron orbital energy difference between both atomic orbitals.[55,58] The M−C bond in CuCN and AgCN mainly shows an ionic character, while both covalent and ionic contribution might be almost equal in case of AuCN.[56-58] The above results may provide some help for us to understand the coordination interaction between FH_2X and MCN. Here FH_2X···MCN can be thought to be formed by the metal atom M simultaneously coordinated with both CN and X. Consequently, it is expected that the binding distance in FH_2X···MCN shows the same change as the M−C bond length. The conclusion that the FH_2X···CuCN complex is more stable than the FH_2X···AgCN one can be explained with the positive MEP on the metal atom, which is 0.1887 au and 0.1419 au in CuCN and AgCN (Fig. 2), respectively. Similarly, the strongest coordination interaction in FH_2X···AuCN is attributed to the prominent relativistic effects of Au atom. Additionally, there is the retrodonation from MCN metal orbital to the X−F anti-bonding orbital and the corresponding E^2 in the AuCN complex is almost twice as much as those in the CuCN and AgCN ones (Table 1), which does not follow the MEP tendency.

Energy decomposition of coordination interaction gives us a visual representation of the physical meaningful components. In FH_2X···CuCN and FH_2X···AgCN, ES term is more negative than POL and DISP ones, thus it is reasonable to explain their difference in stability with the positive MEP on both metal atoms. A detailed comparison for the three attractive terms (ES, POL, and DISP) between FH_2X···CuCN and FH_2X···AgCN indicates that the difference of ES is small, POL is less negative in FH_2X···CuCN than

that in $FH_2X\cdots AgCN$, and DISP is more negative in the former than that in the latter. Namely, the polarization and dispersion energies also have important contribution to the stability of the two complexes. However, in $FH_2X\cdots AuCN$, the POL contribution exceeds the ES one and the former is obviously larger than that in $FH_2X\cdots CuCN$ and $FH_2X\cdots AgCN$ with comparison to other terms. The relatively large POL means that the molecular orbitals undergo significant changes in their shapes, which is typical in the formation of a covalent bond. For the coordination interaction with the same X atom, the DISP term is more negative in order of X···Ag < X···Au < X···Cu, however, the X···M distance is shorter in the same order. The smaller DISP in the X···Au interaction than in the X···Cu one may be attributed to the fact that the electronegativity of Au is larger than that of Cu. The stronger X···Cu interaction is responsible for the larger DISP in the X···Cu interaction than the weaker X···Ag one.

The existence of both pnicogen bond and coordination interaction is also characterized by the presence of bond critical point (BCP) between the two molecular pairs. Consistent with the strength of the coordination interaction and pnicogen bond, the electron density at the X···M BCP is much larger than that at the X···N BCP (Table 1), although both types of BCPs are different in nature. Moreover, the energy densities at both types of BCPs are negative, indicating the nature of partially covalent bond for both pnicogen bond and coordination interaction.[60]

Upon complexation, there is net charge transfer between the two molecules, which can be measured with the sum of charge on all atoms of FH_2X (Table 1). In the pnicogen bond, the charge on FH_2X is negative. This means that the charge moves from

NH_3 to FH_2X, consistent with the fact that NH_3 and FH_2X act as the electron donor and acceptor in the pnicogen bond, respectively. However, in the coordination interaction, the charge on FH_2X is positive, indicating that FH_2X plays the role of electron donor. It is also found that the charge transfer in the coordination interaction is much larger than that in the pnicogen bond. It is expected that there is an orbital interaction between LP_X of FH_2X and BD^*_{C-M} of MCN in the coordination interaction, where LP_X is the lone pair orbital on the X atom and BD^*_{C-M} denotes the C-M anti-bonding orbital. However, this orbital interaction is not analyzed for the coordination interaction because it is not detected in most complexes of MCN with the formation of X−M bond. According to the formation mechanism of coordination bond, there should exist another type of orbital interaction corresponding to the back-donating bond. Actually, such orbital interaction of $LP_M \rightarrow BD^*_{F-X}$ is present in $FH_2X\cdots MCN$, and it becomes stronger in the order of Ag < Cu < Au. Furthermore, the positive charge on FH_2X shows that the $LP_X \rightarrow BD^*_{C-M}$ orbital interaction is stronger than that of $LP_M \rightarrow BD^*_{F-X}$ in the coordination interaction.

3.2. FH_2X (X = P, As) simultaneously acting as the electron donor and acceptor

The structures of ternary complexes $H_3N\cdots FH_2X\cdots MCN$ (X = P and As; M = Cu, Ag, and Au) with C_s symmetry are illustrated in Fig. 3. The structures of the two molecular pairs of $FH_2X\cdots NH_3$ and $FH_2X\cdots MCN$ in the ternary complexes are similar to those in the optimized binary complexes, although the angle F−X···N becomes a little larger and the F−X···M one is smaller in most ternary complexes (Table S2). In the ternary complexes, the σ−hole on the X atom of FH_2X interacts with the lone pair of the nitrogen base and the lone pair on the X atom is paired with the metal atom of MCN

simultaneously. The F−P bond is contracted in the trimer of FH_2P and the F−As bond is stretched in the trimer of FH_2As (Table S3). This is due to the fact that FH_2P is better electron donor and worse electron acceptor than FH_2As. However, both F−P and F−As stretch vibrations display a small red shift in the trimers. The changes of both bonds in the trimers are smaller those in the corresponding dimers. The elongation of C−M bond becomes smaller in the trimers, and the elongation of C≡N bond is almost not changed in the trimers.

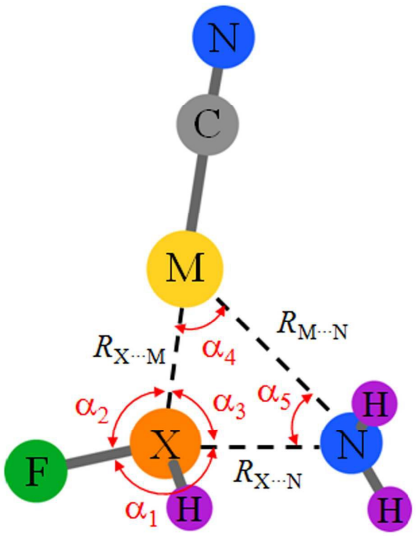

Fig. 3 Scheme of ternary complex $H_3N\cdots FH_2X\cdots MCN$ (X = P and As; M = Cu, Ag, and Au).

The corresponding binding distances in the ternary complexes are gathered in Table 3. Clearly, in the ternary complexes, the X···N distance is shorter but the X···M one is longer with comparison to those in the corresponding binary complexes, as illustrated in the last two columns of Table 3. However, the interaction energy of pnicogen bond in the ternary complex is less negative than that in the corresponding binary one (Table S4). It is obvious that the less negative interaction energy of pnicogen bond does not cause a longer X···N distance in the ternary complex. So a question occurs: which is more

reliable to estimate the change of pnicogen bonding strength, the binding distance or the interaction energy? We firstly analyze the effect of the calculating method on the interaction energy in the ternary complex. The interaction energy of pnicogen bond in the ternary complex is calculated by subtracting the interaction energy between NH_3 and MCN from the interaction energy between $FH_2X\cdots MCN$ and NH_3. Here the interaction energy between $FH_2X\cdots MCN$ and NH_3 is obtained on base of the energies of the optimized monomers and dyads, while the interaction energy between NH_3 and MCN is calculated with the geometries of the monomers and dyad in the ternary complex. The latter interaction energy is in the range of -7.7 ~ -10.3 kcal/mol (Table S4), which is large enough not to be neglected. Unluckily, these values are an approximation because the charge densities on the monomers and dyads during the calculation of the interaction energy between NH_3 and MCN are different from those in the ternary complex. Thus we think that the results of binding distances are more reliable. Namely, in the ternary complex, the pnicogen bond is stronger but the coordination interaction is weaker relative to those in the binary complex. A further evidence for such change of both pnicogen bond and coordination interaction strength is provided by the change of electron density at the X···N and X···M BCPs in the ternary complex. It is found from Table 4 that the electron density at the X···N BCP is increased and that at the X···M BCP is decreased. Obviously, the change of electron density at the intermolecular BCP is consistent with the change of binding distance in the ternary complex. It was demonstrate that the electron density is a good method for estimating the strength of noncovalent interaction.[61] Hence, it is right for the conclusion on the change of

interaction strength based on the change of binding distance. That is, the stronger coordination interaction strengthens the weaker pnicogen bond, while the presence of pnicogen bond seems to weaken the coordination interaction in the ternary complex. However, this conclusion is converse to that in the homotrimers of $(PH_3)_3$[40] and $(PH_2X)_3$ with X = F, Cl, OH, NC, CN,CH_3, H, and BH_2[41] as well as in the heterotrimers LA···FH_2P···FH_2N and LA···H_3P···NH_3 (LA = NCH, ClH, FH, FCl, and HLi),[42] where the pnicogen atoms also play the dual role of both Lewis acid and base. The possible reason for this contradiction is that MCN also acts as the dual role of Lewis acid and base in the X···M interaction. In the following section, we try to give a logical explanation for this abnormal result.

Table 3 Binding distances (R, Å) in the heterotrimers and their change relative to the corresponding heterodimers (ΔR, Å)

	$R_{X\cdots N}$	$R_{X\cdots M}$	$R_{M\cdots N}$	$\Delta R_{X\cdots N}$	$\Delta R_{X\cdots M}$
H_3N···FH_2P···CuCN	2.543	2.108	2.975	-0.060	0.025
H_3N···FH_2P···AgCN	2.502	2.290	3.114	-0.101	0.022
H_3N···FH_2P···AuCN	2.497	2.232	3.119	-0.106	0.030
H_3N···FH_2As···CuCN	2.506	2.200	3.083	-0.092	0.022
H_3N···FH_2As···AgCN	2.489	2.375	3.215	-0.109	0.016
H_3N···FH_2As···AuCN	2.464	2.328	3.192	-0.134	0.024

Table 4 Electron density (ρ, au), Laplacian ($\nabla^2\rho$, au), and energy density (H, au) at the intermolecular BCPs in the heterotrimers

	$\rho_{X\cdots N}$	$\nabla^2\rho_{X\cdots N}$	$H_{X\cdots N}$	$\rho_{X\cdots M}$	$\nabla^2\rho_{X\cdots M}$	$H_{X\cdots M}$
H_3N···FH_2P···CuCN	0.032	0.067	-0.004	0.116	0.139	-0.066
H_3N···FH_2P···AgCN	0.034	0.070	-0.005	0.103	0.145	-0.046
H_3N···FH_2P···AuCN	0.034	0.071	-0.005	0.130	0.057	-0.075
H_3N···FH_2As···CuCN	0.037	0.084	-0.004	0.101	0.122	-0.052
H_3N···FH_2As···AgCN	0.038	0.087	-0.005	0.091	0.127	-0.037
H_3N···FH_2As···AuCN	0.040	0.090	-0.005	0.112	0.080	-0.057

Firstly, we pay our attention on the change of the most positive MEP on the σ-hole of the X atom in $FH_2X\cdots MCN$ and the most negative MEP on the lone pair of the X atom in $FH_2X\cdots NH_3$ (Table 5). One can see that the most positive MEP on the σ-hole of the X atom is increased in $FH_2X\cdots MCN$, thus this σ-hole is a stronger Lewis acid in $FH_2X\cdots MCN$ than that in FH_2X and forms a stronger pnicogen bond with NH_3 in the ternary complex. The rationality with the electrostatic potential to explain the enhancement of pnicogen bond in the ternary complex is in view of the fact that the electrostatic energy is dominant in the formation of pnicogen bond. Likely, the most negative MEP on the lone pair of the X atom also becomes more negative in $FH_2X\cdots NH_3$ than that in FH_2X, giving rise to a hint that the X atom in $FH_2X\cdots NH_3$ would form a stronger coordination interaction with MCN. However, this is inconsistent with the weakening of coordination interaction in the ternary complex, partly because the polarization and dispersion energies are also important in the formation of coordination interaction. Secondly, we focus on the change of occupancy on the lone pair of the X atom in $FH_2X\cdots NH_3$ (Table 5). Obviously, this occupancy is decreased in the dyad, indicating a weaker Lewis base for the lone pair on the X atom in $FH_2X\cdots NH_3$. The decrease of the occupancy on the lone pair of the X atom in $FH_2X\cdots NH_3$ is ascribed to the presence of the orbital interaction between the lone pair of the X atom and the N−H anti-bonding orbital of NH_3. This decrease supports the weakening of coordination interaction in the ternary complex. Thirdly, we are interested in the charges on the three molecules in the ternary complexes (Table 6). Like that in the binary complex, the charge on NH_3 is positive and that on MCN is negative in the ternary complex. Clearly,

the positive charge on NH_3 is increased in the ternary complex, also providing an explanation for the enhancement of pnicogen bond based on the Scheiner' description for the formation of pnicogen bond.[5] The charge on FH_2X is positive in the ternary complex, which is a combinative result of FH_2X in the pnicogen bond and coordination interaction (Table 1). The negative charge on MCN is decreased in the ternary complexes of CuCN and AgCN but is increased in those of AuCN. It should be pointed out that the negative charge on MCN is jointly caused by the coordination interaction and the M···N interaction between MCN and NH_3. So the change of the charge on MCN can not accurately reflect the change of the coordination interaction in the ternary complex. Finally, we fall back on the orbital interactions of $LP_N \rightarrow BD^*_{F\text{-}X}$ and $LP_M \rightarrow BD^*_{F\text{-}X}$ (Table 6). The former orbital interaction becomes stronger in the ternary complex relative to the corresponding dyad, while the latter one has a reverse change. Both of them show a consistent change with the binding distances.

Table 5 The most positive MEP (V_{max}, au) on the σ-hole of X in $FH_2X\cdots MCN$, the most negative MEP (V_{min}, au) on the X atom in $FH_2X\cdots NH_3$, and the occupancy (n, e) on the lone pair orbital of the X atom in $FH_2X\cdots NH_3$ and FH_2X (in parentheses)

	$V_{max,X}$
$FH_2P\cdots CuCN$	0.0977
$FH_2P\cdots AgCN$	0.1042
$FH_2P\cdots AuCN$	0.0961
$FH_2As\cdots CuCN$	0.1092
$FH_2As\cdots AgCN$	0.1136
$FH_2As\cdots AuCN$	0.1078
	$V_{min,,X}$
$FH_2P\cdots NH_3$	-0.0316
$FH_2As\cdots NH_3$	-0.0234
	n

$FH_2P\cdots NH_3$	1.9926(1.9967)
$FH_2As\cdots NH_3$	1.9932(1.9965)

Table 6 Charges (q, e) on three molecules and second-order perturbation energy (E^2, kcal/mol) in the ternary complexes

	q_{NH3}	q_{FH2X}	q_{MCN}	E^2(a)	E^2(b)	E^2(c)
$H_3N\cdots FH_2P\cdots CuCN$	0.0848	0.1534	-0.2382	18.2(14.8)	3.1(4.7)	1.77
$H_3N\cdots FH_2P\cdots AgCN$	0.0913	0.1253	-0.2066	20.4	3.6(4.4)	1.08
$H_3N\cdots FH_2P\cdots AuCN$	0.0904	0.2114	-0.3018	17.1	7.2(8.5)	0.72
$H_3N\cdots FH_2As\cdots CuCN$	0.0955	0.1521	-0.2477	25.1(19.0)	3.8(4.5)	1.19
$H_3N\cdots FH_2As\cdots AgCN$	0.0985	0.1106	-0.2091	26.4	3.7(4.4)	0.71
$H_3N\cdots FH_2As\cdots AuCN$	0.1022	0.2044	-0.3066	22.4	7.0(8.1)	0.42

Note: E^2(a), E^2(b), and E^2(c) correspond to the orbital interactions of $LP_N\rightarrow BD^*_{F\text{-}X}$, $LP_M\rightarrow BD^*_{F\text{-}X}$, and $LP_N\rightarrow BD^*_{M\text{-}C}$, respectively. Data in parentheses are from the corresponding dyads.

In the above analyses, the M···N interaction between MCN and NH_3 is considered. Here we provide some evidences for its existence in the ternary systems and investigate its effect on the coordination interaction. The M···N distance is smaller than the sum of the van der Waals radii of the respective atoms (3.4 Å for N and Cu, 3.5 Å for N and Ag, and 3.5 Å for N and Au).[62] The NBO analyses indicate that there is the orbital interaction between the N lone pair of NH_3 and the C−M anti-bonding orbital of MCN. The coinage metal in MCN acts as a double Lewis acid in the X···M and M···N interactions. Consequently, the presence of the M···N interaction in the ternary complex also has contribution to the weakening of the X···M interaction.

a) $FH_2P\cdots NH_3$

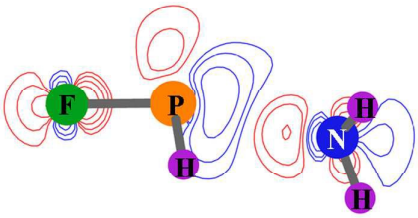

b) $FH_2P\cdots AgCN$

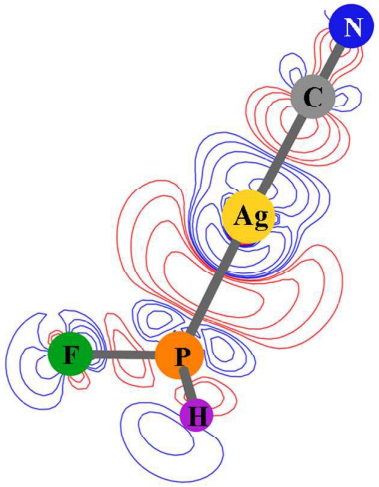

c) $H_3N\cdots FH_2P\cdots AgCN$

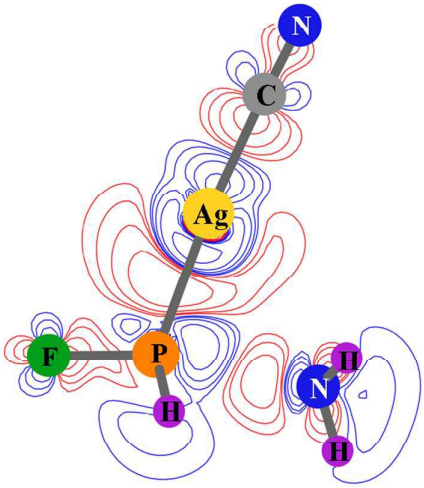

Fig. 4 Electron density difference maps of $FH_2P\cdots NH_3$, $FH_2P\cdots AgCN$, and $H_3N\cdots FH_2P\cdots AgCN$ complexes. The red lines represent the concentration of electron density and the blue ones are the regions with reduced electron density.

To have an insight into the electron redistribution during the formation of complexes, electron density difference (EDD) maps are depicted in Fig. 4, taking $FH_2P\cdots NH_3$, $FH_2P\cdots AgCN$ and $H_3N\cdots FH_2P\cdots AgCN$ for examples. The red lines represent the concentration of electron density and the blue ones are the regions with reduced electron density. For the pnicogen-bonded dyad of $FH_2P\cdots NH_3$, a red increase occurs in the region of the lone pair on the P and N atoms, accompanied with a blue decrease area on the σ-hole of the P atom. For the coordination-bonded dyad of $FH_2P\cdots AgCN$, there is an electron deficit around the P and Ag atoms, and this deficit is separated by a red increase of electron density. This confirms the dual roles of Lewis acid and base for both P and Ag atoms in the coordination interaction. In the ternary complex of $H_3N\cdots FH_2P\cdots AgCN$, the main pattern of the redistribution of pnicogen bond and coordination bond still remains, but some differences are observed. The red increase area between the P and Ag atom is asymmetrical due to the effect of the M···N interaction. The electron concentration area becomes bigger on the lone pair of NH_3, whereas the electron deficit region is smaller around the Ag atom, respectively indicative of the enhancement of pnicogen bond and the weakening of the covalent interaction.

4. Conclusions

Ternary complexes $H_3N\cdots FH_2X\cdots MCN$ (X = P and As; M = Cu, Ag, and Cu) and the corresponding binary complexes have been studied. The pnicogen bond occurs between the σ−hole on the X atom of FH_2X and the lone pair on the N atom of NH_3, mainly driven by the electrostatic interaction and the charge transfer from the nitrogen base to the F−P σ* anti-bond orbital. The coordination interaction shows a nature of covalent

bond, characterized with the orbital interactions of both $LP_N \rightarrow BD^*_{F\text{-}X}$ and $LP_M \rightarrow BD^*_{F\text{-}X}$. The coordination interaction becomes stronger in the order of Ag < Cu < Au and As < P. The abnormality of gold atom is mainly attributed to its large relativistic effect. In the ternary complexes of $H_3N\cdots FH_2X\cdots MCN$, the pnicogen bond is strengthened but the coordination interaction becomes weaker. The weakening of coordination interaction is due to the dual roles of Lewis acid and base for the pnicogen and coinage metal atoms, evidenced by the change of the orbital interactions and the occupancy on the lone pair of the pnicogen bond.

Acknowledgements

This work was supported by the Outstanding Youth Natural Science Foundation of Shandong Province (JQ201006), the Program for New Century Excellent Talents in University (NCET-2010-0923), and the Students' Science and Technology Innovation of Yantai University (130516).

References

1 S. Zahn, R. Frank, E. Hey-Hawkins and B. Kirchner, *Chem. Eur. J.*, 2011, **17**, 6034–6038.

2 S. Scheiner, *Phys. Chem. Chem. Phys.*, 2011, **13**, 13860–13872.

3 S. Scheiner, *J. Chem. Phys*., 2011, **134**, 164313.

4 M. Solimannejad, M. Gharabaghi and S. Scheiner, *J. Chem. Phys.*, 2011, **134**, 024312.

5 S. Scheiner, *J. Chem. Phys.*, 2011, **134**, 094315.

6 J. E. Del Bene, I. Alkorta, G. Sanchez-Sanz and J. Elguero, *Chem. Phys. Lett.*, 2011, **512**, 184–187.

7 S. Scheiner and U. Adhikari, *J. Phys. Chem. A*, 2011, **115**, 11101–11110.

8 J. E. Del Bene, I. Alkorta, G. Sanchez-Sanz and J. Elguero, *J. Phys. Chem. A*, 2012,

116, 3056−3060.

9 S. Scheiner, *Acc. Chem. Res.*, 2013, **46**, 280–288.

10 J. E. Del Bene, I. Alkorta, G. Sanchez-Sanz and J. Elguero, *J. Phys. Chem. A*, 2013, **117**, 183−191.

11 S. Scheiner, *CrystEngComm*, 2013, **15**, 3119–3124.

12 A. Bauzá, D. Quiñonero, P. M. Deyà and A. Frontera, *Phys. Chem. Chem. Phys.*, 2012, **14**, 14061–14066.

13 A. Bauzá, D. Quiñonero, P. M. Deyà and A. Frontera, *CrystEngComm*, 2013, **15**, 3137–3144.

14 X. L. An, R. Li, Q. Z. Li, X. F. Liu, W. Z. Li and J. B. Cheng, *J. Mol. Model*., 2012, **18**, 4325–4332.

15 H. Y. Xu, W. Wang and J. W. Zou, *Acta. Chim. Sinica.,* 2013, **71**, 1175–1182.

16 J. E. Del Bene, I. Alkorta and J. Elguero, *Theor. Chem. Acc.*, 2014, **133**, 1464/1–1464/9.

17 Q. Z. Li, R. Li, X. F. Liu, W. Z. Li and J. B. Cheng, *J. Phys. Chem. A,* 2012, **116**, 2547–2553.

18 I. Alkorta, J. Elguero and M. Solimannejad, *J. Phys. Chem. A*, 2014, **118**, 947−953.

19 J. E. Del Bene, I. Alkorta and J. Elguero, *J. Phys. Chem. A*, 2014, **118**, 3386–3392.

20 Y. S. Chen, L. F. Yao and X. F. Lin, *Comput. Theor. Chem.*, 2014, **1036**, 44–50.

21 A. Bauzá, I. Alkorta, A. Frontera and J. Elguero, *J. Chem. Theory Comput.*, 2013, **9**, 5201−5210.

22 T. Clark, M. Hennemann, J. S. Murray and P. Politzer, *J. Mol. Model.*, 2007, **13**, 291−296.

23 S. J. Grabowski, *Chem. Eur. J.,* 2013, **19**, 14600−14611.

24 J. E. Del Bene, I. Alkorta and J. Elguero, *J. Phys. Chem. A*, 2013, **117**, 11592−11604.

25 I. Alkorta, G. Sánchez-Sanz and J. Elguero, *J. Phys. Chem. A*, 2014, **118**, 1527−1537.

26 G. Sánchez-Sanz, C. Trujillo, M. Solimannejad, I. Alkorta and J. Elguero, *Phys. Chem. Chem. Phys.*, 2013, **15**, 14310−14318.

27 I. Alkorta and J. Elguero, *J. Phys. Chem. A*, 2013, **117**, 10497−10503.

28 J. E. Del Bene, I. Alkorta and J. Elguero, *J. Phys. Chem. A*, 2013, **117**, 6893−6903.

29 S. Scheiner, *J. Phys. Chem. A,* 2011, **115**, 11202–11209.

30 S. Scheiner, *Chem. Phys.*, 2011, **387**, 79–84.

31 J. E. Del Bene, I. Alkorta, G. Sanchez-Sanz and J. Elguero, *J. Phys. Chem. A,* 2011, **115**, 13724–13731.

32 Q.Z. Li, N.N. Wang, Q. Zhou, S.Q. Sun and Z.W. Yu, *Appl. Spectrosc*. 2008, **62**, 166–170.

33 Q. Z. Li, R. Li, X. F. Liu, W. Z. Li and J. B. Cheng, *ChemPhysChem*, 2012, **13**, 1205–1212.

34 I. Alkorta, G. Sánchez-Sanz and J. Elguero, *J. Chem. Theory Comput.*, 2012, **8**, 2320−2327.

35 J. E. Del Bene, *J. Phys. Chem. A*, 2012, **116**, 9205−9213.

36 M. D. Esrafili, P. Fatehi and M. Solimannejad, *Comput. Theor. Chem.*, 2014, 1034, 1–6.

37 Q. Z. Li, H. Y. Zhuo, X. Yang, J. B. Cheng, W. Z. Li and R. E. Loffredo, *ChemPhysChem*, 2014, **15**, 500–506.

38 Y. X. Lu, J. W. Zou, H. Q. Wang, Q. S. Yu, H. X. Zhang and Y. J. Jiang, *J. Phys. Chem. A*, 2005, **109**, 11956–11961.

39 P. P. Zhou, W. Y. Qiu, S. Liu and N. Z. Jin, *Phys. Chem. Chem. Phys.*, 2011, **13**, 7408–7418.

40 U. Adhikari and S. Scheiner, *J. Chem. Phys.*, 2011, **135**, 184306.

41 I. Alkorta, J. Elguero and J. E. Del Bene, *J. Phys. Chem. A*, 2013, **117**, 4981−4987.

42 J. E. Del Bene, I. Alkorta, G. Sánchez-Sanz and J. Elguero, *J. Phys. Chem. A*, 2013, **117**, 3133−3141.

43 Y. P. Zhou, M. Zhang, Y. H. Li, Q. R. Guan, F. Wang, Z. J. Lin, C. K. Lam, X. L. Feng and H. Y. Chao, *Inorg. Chem.*, 2012, **51**, 5099–5109.

44 K. Peterson, B. Shepler, D. Figgen and H. Stoll, *J. Chem. Phys.* **2007**, 126, 12410 (1-12).

45 S. F. Boys and F. Bernardi, *Mol. Phys.*, 1970, **19**, 553−566.

46 M. J. Frisch, G. W. Trucks, H. B. Schlegel, G. E. Scuseria, M. A. Robb, J. R. Cheeseman, G. Scalmani, V. Barone, B. Mennucci, G. A. Petersson, H. Nakatsuji, M. Caricato, X. Li, H. P. Hratchian, A. F. Izmaylov, J. Bloino, G. Zheng, J. L. Sonnenberg, M. Hada, M. Ehara, K. Toyota, R. Fukuda, J. Hasegawa, M. Ishida, T. Nakajima, Y. Honda, O. Kitao, H. Nakai, T. Vreven, J. J. A. Montgomery, J. E. Peralta, F. Ogliaro, M. Bearpark, J. J. Heyd, E. Brothers, K. N. Kudin, V. N. Staroverov, R. Kobayashi, J. Normand, K. Raghavachari, A. Rendell, J. C. Burant, S. S. Iyengar, J. Tomasi, M. Cossi, N. Rega, J. M. Millam, M. Klene, J. E. Knox, J. B. Cross, V. Bakken, C. Adamo, J. Jaramillo, R. Gomperts, R. E. Stratmann, O. A. Yazyev, J. Austin, R. Cammi, C. Pomelli, J. W. Ochterski, R. L. Martin, K. Morokuma, V. G. Zakrzewski, G. A. Voth, P. Salvador, J. J. Dannenberg, S. A. Dapprich, D. Daniels, O. Farkas, J. B. Foresman, J. V. Ortiz, J. Cioslowski and D. J. Fox, Gaussian 09, Revision A.02, Gaussian, Inc., Wallingford, CT, 2009.

47 F. A. Bulat, A. Toro-Labbé, T. Brinck, J. S. Murray and P. Politzer, *J. Mol. Model*., 2010, **16**, 1679−1691.

48 R. F. W. Bader, AIM2000 Program, v 2.0; McMaster University, Hamilton, Canada, 2000.

49 L. Tian, *Multiwfn Version 2.01*; http://Multiwfn.codeplex.com.

50 A. E. Reed, L. A. Curtiss and F. Weinhold, *Chem. Rev*., 1988, **88**, 899−926.

51 P. F. Su and H. Li, *J. Chem. Phys*., 2009, **131**, 014102.

52 M. W. Schmidt, K. K. Baldridge, J. A. Boatz, S. T. Elbert, M. S. Gordon, J. H. Jensen, S. Koseki, N. Matsunaga, K. A. Nguyen, S. J. Su, T. L. Windus, M. Dupuis and J. A. Montgomery, *J. Comput. Chem.*, 1993, **14**, 1347–1363.

53 J. E. Del Bene, I. Alkorta, G. Sanchez-Sanz and J. Elguero, *J. Phys. Chem. A*, 2011, **115**, 13724–13731.

54 M. Gao, X. Yang, J. B. Cheng, Q. Z. Li, W. Z. Li and R. E. Loffredo, *ChemPhysChem*, 2013, **14**, 3341–3347.

55 X. Wu, Z. B. Qin, H. Xie, R. Cong, X. H. Wu, Z. C. Tang and H. J. Fan, *J. Phys. Chem. A*, 2010, **114**, 12839–12844.

56 O. Dietz,V. M. Rayón and G. Frenking, *Inorg. Chem.*, 2003, **42**, 4977−4984.

57 C. J. Nelin, P. S. Bagus and M. R. Philpott, *J. Chem. Phys.*, 1987, **87**, 2170−2176.

58 D. K. Lee, I. S. Lim, Y. S. Lee and G. H. Jeung, *Int. J. Mass Spectrom.,* 2007, **271**, 22−29.

59 P. Pyykkö, *Chem. Rev.*, 1988, **88**, 563−594.

60 I. Rozas, I. Alkorta and J. Elguero, *J. Am. Chem. Soc.*, 2000, **122**, 11154–11161.

61 P. Lipkowski, S. J. Grabowski, T. L. Robinson and J. Leszczynski, *J. Phys. Chem. A,* 2004, **108**, 10865–10872.

62 Y. V. Zefirov, *Russ. J. Inorg. Chem.*, 2000, **45**, 1552–1554.